Upper-stratospheric ozone trends 1979-1998

M. J. Newchurch, Lane Bishop, Derek Cunnold, Lawrence E. Flynn, Sophie Godin, Stacey Hollandsworth Frith, Lon Hood, Alvin J. Miller, Sam Oltmans, William Randel, et al.

JOURNAL OF GEOPHYSICAL RESEARCH, VOL. 105, NO. D11, PAGES 14,625–14,636, JUNE 16, 2000

Upper-stratospheric ozone trends 1979-1998

M. J. Newchurch,[1,2] Lane Bishop,[3] Derek Cunnold,[4] Lawrence E. Flynn,[5] Sophie Godin,[6] Stacey Hollandsworth Frith,[7] Lon Hood,[8] Alvin J. Miller,[9] Sam Oltmans,[10] William Randel,[11] Gregory Reinsel,[12] Richard Stolarski,[7] Ray Wang,[4] and Eun-Su Yang[1], Joseph M. Zawodny[13]

Abstract. Extensive analyses of ozone observations between 1978 and 1998 measured by Dobson Umkehr, Stratospheric Aerosol and Gas Experiment (SAGE) I and II, and Solar Backscattered Ultraviolet (SBUV) and (SBUV)/2 indicate continued significant ozone decline throughout the extratropical upper stratosphere from 30-45 km altitude. The maximum annual linear decline of -0.8±0.2 % $yr^{-1}(2\sigma)$ occurs at 40 km and is well described in terms of a linear decline modulated by the 11-year solar variation. The minimum decline of -0.1±0.1% $yr^{-1}(2\sigma)$ occurs at 25 km in midlatitudes, with remarkable symmetry between the Northern and Southern Hemispheres at 40 km altitude. Midlatitude upper-stratospheric zonal trends exhibit significant seasonal variation (±30% in the Northern Hemisphere, ±40% in the Southern Hemisphere) with the most negative trends of –1.2% yr^{-1} occurring in the winter. Significant seasonal trends of –0.7 to –0.9% yr^{-1} occur at 40 km in the tropics between April and September. Subjecting the statistical models used to calculate the ozone trends to intercomparison tests on a variety of common data sets yields results that indicate the standard deviation between trends estimated by 10 different statistical models is less than 0.1% yr^{-1} in the annual-mean trend for SAGE data and less than 0.2% yr^{-1} in the most demanding conditions (seasons with irregular, sparse data) [*World Meteorological Organization (WMO)*, 1998]. These consistent trend results between statistical models together with extensive consistency between the independent measurement-system trend observations by Dobson Umkehr, SAGE I and II, and SBUV and SBUV/2 provide a high degree of confidence in the accuracy of the declining ozone amounts reported here. Additional details of ozone trend results from 1978 to 1996 (2 years shorter than reported here) along with lower-stratospheric and tropospheric ozone trends, extensive intercomparisons to assess relative instrument drifts, and retrieval algorithm details are given by *WMO* [1998].

1. Introduction

Substances of anthropogenic origin, such as chlorofluorocarbons (CFCs) and bromine-containing organic volatile compounds, cause stratospheric ozone depletion [*WMO*, 1999]. In the upper stratosphere the primary mechanism by which CFCs affect ozone is through gas-phase reactions involving chlorine radicals. Ozone changes in this region of the atmosphere provide a test of our understanding of these gas-phase reactions. Previous studies of stratospheric ozone trends [*WMO*, 1995; *DeLuisi et al.*, 1994; *McPeters et al.*, 1994; *Reinsel et al.*, 1994; *Rusch et al.*, 1994; *Miller et al.*, 1995, 1996] are summarized by *Harris et al.* [1997]. These studies found that ozone amounts from approximately 1979 to 1991 declined at the rate of 0.5-1.0% yr^{-1} in northern midlatitudes in the altitude region of maximum active chlorine (35-45 km). Those trend estimates were reasonably consistent in the three measurement systems: Dobson Umkehr, Stratospheric Aerosol and Gas Experiment (SAGE) I/II, and Solar Backscattered Ultraviolet (SBUV). As previously noted by *Hood et al.* [1993] using NIMBUS-7 SBUV observations, the altitude-latitude structure and the seasonal structure of the measured ozone trends provide excellent tests of our theoretical understanding of chlorine-catalyzed ozone destruction [*Solomon and Garcia*, 1984; *Kaye and Rood*, 1989] and the measured latitudinal distribution of ClO [*Aellig et al.*, 1996; *Waters et al.*, 1996]. Subsequent analyses of SAGE I/II trends through the same period employing an altitude correction for the SAGE I observations [*Wang et al.*, 1996] reconciled differences between SAGE I/II and SBUV trends that had been present in the tropical lower stratosphere. Subsequent analysis of combined SBUV and SBUV/2 (SBUV(/2)) trends [*Hollandsworth et al.*, 1995], extended through 1994, did not substantially change that general agreement. These upper-stratospheric trends exhibited latitudinal and seasonal variations such that the trends were more

[1]Department of Atmospheric Science, University of Alabama in Huntsville.
[2]Also at National Center for Atmospheric Research, Boulder, Colorado.
[3]Allied Signal Corporation, Buffalo, New York.
[4]School of Earth and Atmospheric Sciences, Georgia Institute of Technology, Atlanta.
[5]NOAA/National Environmental Satellite Data and Information Service, Silver Spring, Maryland.
[6]Service d'Aeronomie, Paris, France.
[7]NASA/Goddard Space Flight Center/Laboratory for Atmospheres, Greenbelt, Maryland.
[8]Lunar and Planetary Laboratory, University of Arizona, Tucson.
[9]NOAA/National Weather Service/Climate Prediction Center, Camp Springs, Maryland.
[10]NOAA/Climate Monitoring and Diagnostics Laboratory, Boulder, Colorado.
[11]National Center for Atmospheric Research, Boulder, Colorado.
[12]Statistics Department, University of Wisconsin, Madison.
[13]NASA/Langley Research Center, Hampton, Virginia.

Paper number 2000JD900037.
0148-0227/00/2000JD900037$09.00

negative in the winter and spring seasons at high latitudes. The trends in the tropical latitudes are less negative throughout the stratosphere and exhibit little seasonal or altitudinal variation. At somewhat lower altitudes (10-20 hPa, ~30 km), these three systems, in addition to ozonesonde observations, concurred in finding a statistically insignificant ozone loss of about -0.2 to -0.4% yr^{-1} over the 1979-1991 period.

The deduced trends in ozone concentration are in general agreement with the latitude and altitude characteristics of theoretical predictions [e.g., *Chandra et al.*, 1995; *Jackman et al.*, 1996] that implicate halogen-induced ozone destruction; however, the magnitude of the model predictions has been somewhat larger than observed trends. These models also significantly overpredict the ClO amounts in the upper stratosphere, leading to overpredictions of ozone destruction. Recent laboratory measurements [*Lipson et al.*, 1997] determine that a minor channel of the reaction OH + ClO produces HCl, effectively reducing the ClO/HCl model excess. Including the HCl branch in model chemistry brings the model ozone-trend predictions in line with observed trends [*WMO*, 1999]. However, the expected ozone recovery could be delayed if the current halogen growth continues into the next decade [*Fraser et al.*, 1999] or interactions between greenhouse-gas increases and radiation slow dynamic transport of tropical air to higher latitudes and increase polar stratospheric cloud formation due to lower temperatures [*Shindell et al.*, 1998]. Then these lower ozone columns will continue to affect surface UVB radiation [*Madronich et al.*, 1998].

Satellite-based instruments provide superior spatial coverage of Earth compared to surface-based Dobson instruments; however, the Dobson records extend many years prior to the satellite records, and these instruments are routinely calibrated. The various satellite instruments have different individual characteristics with respect to long-term calibration stability, global coverage, vertical resolution, and sensitivity to contamination by stratospheric aerosol. The solar-occultation instruments, SAGE I (which operated from 1979 to 1981) and SAGE II (1984 to present), employ atmospheric limb extinction at several wavelengths during sunrise and sunset events. They have good long-term stability because they are able to reference their atmospheric measurements to the exoatmospheric sun before sunset and after sunrise for each vertical-profile measurement. Their vertical resolution is the best of all satellite techniques (of the order of 1 km). However, their spatial coverage is relatively poor because of the requirement of an orbital solar sunrise or sunset. Limb viewing in the visible/near-infrared is also subject to contamination by volcanic aerosols in the observation slant column, thereby making the ozone measurements below ~20 km questionable [*Cunnold et al.*, 2000b]. The nadir-viewing backscatter ultraviolet (BUV) type instruments SBUV (1978-1990) and SBUV/2 (1989-1994), which we denote as SBUV(/2) when referring to both instruments as a series from 1978-1994), have good global coverage for ozone profiles above ~25 km but are subject to calibration uncertainties and the possibility of long-term drift and have relatively coarse vertical resolution. Aerosol contamination is a problem for these instruments immediately following a major volcanic eruption.

The overall purpose of this paper is to extend by 2 years and to provide additional interpretation of the salient results of the analyses of WMO [1998], which reported extensive details on the instrument characteristics, relative instrument drifts, and trends in both the stratosphere and troposphere. In addition to extending the analyzed time period, we also reanalyze the Dobson Umkehr record in a more consistent manner between two independent groups and provide significantly more information on the adequacy of the model fits to the Umkehr, SAGE I/II, and SBUV(/2) data series. *Cunnold et al.* [2000a] report on the uncertainties in these upper-stratospheric trends. *Cunnold et al.* [2000b] report trends in the lower stratosphere. *Logan et al.* [1999] report the tropospheric and lower-stratospheric trends derived from ozonesonde observations. *Randel et al.* [1999] report the overview of trends and comparisons at all altitudes.

Section 2 compares the results of the statistical trend models employed for the calculations. Section 3 presents the vertical profiles of ozone trends in the upper stratosphere (20-50 km). The conclusions appear in section 4.

2. Statistical Models

A wide variety of statistical models has been used to derive trends in stratospheric ozone and to determine the effects on ozone of other variables such as the solar cycle and the quasi-biennial oscillation (QBO). The 1988 Trends Assessment [*WMO*, 1989, chapter 2] briefly intercompares results from a few of these statistical models. While variations in the statistical model or in the ancillary variables (solar, QBO, nuclear effect, etc.) had relatively minor effects on the calculated ozone trends, at least for total ozone, questions continue to arise as to how much of the difference in the trends or standard errors is due to differences in data used and how much is due to the differences in the statistical model construction. To address those questions, researchers compared the statistical-trend calculations of a number of models on common sets of actual ozone data. The results of using three widely different test data series for the intercomparisons reported in *WMO* [1998] illustrate the statistical model issues.

In addition to QBO and faster timescale dynamical variability, decadal variations are a ubiquitous feature of ozone observations [*Randel et al.*,1998]. Terms with periods less than ~2 years have little influence on calculating or interpreting trends. However, some of the observed decadal changes (e.g., volcanic eruptions) are approximately in phase with the solar cycle, suggesting a solar forcing mechanism. Current model calculations of the solar effect show some inconsistencies with observations (in terms of magnitude and lower-stratospheric response), and this inconsistency limits confidence in our detailed understanding of ozone trends. There is also likely a confusion of solar and volcanic signals for the recent record. Although these effects have relatively small impacts on trend estimates, they do limit our ability to interpret decadal variability.

We use one form of statistical model as a context for discussing the statistical issues in the intercomparison of models. For some additional discussion of the terms and statistical issues, see *Bojkov et al.* [1990] and *WMO* [1998]. Let y_t represent monthly ozone values for one of the test series; in some cases y_t is missing for some months, and this problem is addressed in the notes below. The statistical model for y_t is of the following form:

y_t = (Monthly mean) + (Monthly trend) + (Solar effect) + (QBO effect) + Noise

or more precisely,

$$y_t = \sum_{i=1}^{12} \mu_i I_{i;t} + \sum_{i=1}^{12} \beta_i I_{i;t} R_t + \gamma_1 Z_{1;t} + \gamma_2 Z_{2;t} + N_t ,$$

where

μ_i ozone mean in month i, i = 1...12 in the instrument's native units (e. g., Dobson Units for TOMS, SBUV, and Umkehr; number density for SAGE);

$I_{i;t}$ indicator series for month i of the year; i.e., 1 if the month corresponds to month i of the year and 0 otherwise;

β_i trend in month i of the year in Dobson units yr^{-1} for TOMS, SBUV, and Umkehr and in number density for SAGE;

R_t linear ramp function measuring years from the first month of the series; equal to $(t-t_o)/12$. For series beginning before 1970, it is often taken to be a ramp function equal to zero for $t < t_o$, where t_o corresponds to 12/69, and then $(t-t_o)/12$ for $t \geq t_o$;

$Z_{1;t}$ solar 10.7 cm flux or MgII series, with γ_1 the associated coefficient;

$Z_{2;t}$ QBO series lagged some appropriate number of months (latitude and altitude dependent), with γ_2 the associated coefficient;

N_t residual noise series.

This is the underlying model used by most researchers; however, such statistical model issues as seasonal variations and weighting, autocorrelation, additional exogenous series, and the form of the trend term are handled differently by different researchers, or even by the same researcher depending upon data features (e.g., if the proportion of missing data is very high). In time series with significant missing data, the calculation of the autoregressive (AR) coefficients will affect the magnitude of the trend uncertainty. Participating researchers reported their trend results, together with notes on their models in the *WMO* [1998, 1999] reports.

To examine the question of how including or neglecting the solar, QBO, and other terms in the statistical models influences the derived trend and standard error estimates (i.e., how sensitive the trend results are to details of other model terms), researchers used models with only a linear-trend component. Comparison to the full-model trend results showed relatively small (~10%) changes in values of the trends. Detailed changes in standard error are expected to be sensitive to location (such as at the equator, where the QBO component is relatively important). However, the overall conclusion is that the trend results are relatively insensitive to inclusion of other terms in the statistical models. This insensitivity is probably because the time series are sufficiently long compared to the ~2 year QBO periodicities. A similar insensitivity of trend results is found concerning the inclusion or neglect of data during the El Chichon and/or Mount Pinatubo time periods for data

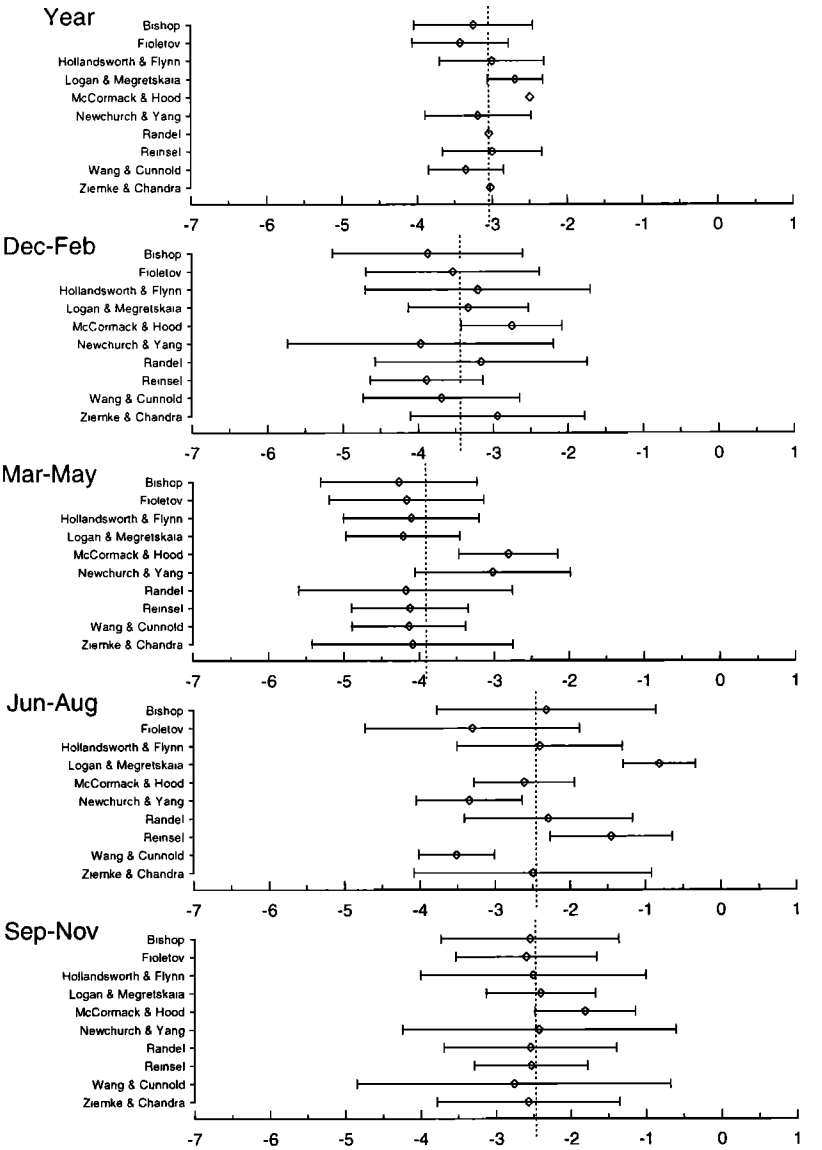

Figure 1. Ozone trend estimates by researcher for SAGE I and II 40.5 km ozone November 1978 - April 1993, 35^0-45^0N. Trends are in 10^{-9} cm^{-3} yr^{-1}. Uncertainty intervals are one standard statistical error. Vertical dotted line is the mean of all researchers' trend estimates (taken from *WMO* [1998 Figure 3.4].

through 1998. In addition, although some degree of collinearity between the solar and aerosol proxies might be expected due to their roughly similar periods, during the period of this study, 1979-1998, we calculate that the collinearity is actually insignificant. This result is corroborated by the fact that the trend estimates and uncertainties from the Dobson Umkehr measurements calculated by two independent methods, aerosol correction before applying the statistical model and aerosol correction by the statistical model, show no systematic difference.

Intercomparison of the statistical models from 10 independent groups computing trends from the Total Ozone Mapping Spectrometer (TOMS) test data with no missing monthly values indicates agreement between models to within 0.015% yr^{-1}, 1 standard deviation (smaller than the average individual model trend uncertainty) in this most benign case (a completely continuous time series). Variations in standard errors among the groups, however, were large enough to give some concern because the variations affect the statistical significance of the calculated trends. For example, because long-term total ozone trends near the equator border on statistical significance [*WMO*, 1995], the lack of proper calculation of standard errors may result in nonsignificant trends' being declared statistically significant or vice versa. The results of the relatively stressing SAGE test (Figure 1) indicate agreement within 0.1% yr^{-1} (1 standard deviation) for annual mean trends.

In the case of a discontinuous time series with irregular seasonal coverage, all models agreed to within 0.1% yr^{-1}, 1 standard deviation, for annual-mean trends and to within 0.2% yr^{-1}, 1 standard deviation, for worst-case seasonal trends with the model-to-model variance less than or equal to the average model-trend uncertainty. A major part of this variance could be attributed to the details of how a particular model handles missing data. Most researchers feel that in such situations, it is better to fit a simpler model to maintain stability, for example, by fitting seasonal trends directly or by reducing the number of harmonic terms for the seasonal trends and possibly also for the seasonal cycle. On the basis of these intercomparisons it seems reasonable to suggest that researchers provide good documentation for the features of their statistical model. Particularly, when any patterns of missing data have strong time-dependent features (e.g., missing monthly periods in the SAGE data), the methods of handling the missing data should be discussed.

This substantial agreement between the various statistical models significantly enhances our confidence in their trend results and uncertainties. Variation with periods equal to or less than the QBO exert little influence on calculated ozone trends and the aerosol effect on the Umkehr observations is well separated from the 11-year solar cycle effect resulting in decadal variations in ozone well partitioned between volcanic and solar-cycle influences.

3. Vertical Profiles of Ozone Trends

3.1. Accounting for Aerosol Effects in Umkehr Observations

The well-known aerosol interference in the Umkehr observations is an optical interference effect on the measurements and not an in situ ozone-aerosol interaction. The following three methods have historically been employed to identify the magnitude of and correction for this aerosol interference: (1) theoretical radiative transfer calculations [*Mateer and DeLuisi*, 1992], (2) statistical calculations (i.e., time series regression models employing exogenous aerosol records) [*DeLuisi et al.*, 1994; *Reinsel et al.*,1999], and (3) comparisons to other ozone measurements [*Newchurch and Cunnold*, 1994].

To correct for the optical interference, the authors of this report employ two methods. Method 1, employed by M.J. Newchurch and E.-S. Yang, uses the coefficients of *Mateer and DeLuisi* [1992] with aerosol data from coincident SAGE II aerosol extinction measurements [*Newchurch and Cunnold*, 1994; *Newchurch et al.*, 1995] along with Garmisch lidar backscatter measurements (H. Jäger, private communication, 1997) for the period prior to 1984. The lidar backscatter measurements are converted to optical depths at 320 nm by regression against SAGE-II coincident measurements from 1984 to 1995. The resulting continuous aerosol time series is then lagged appropriately to correct Umkehr data at various latitudes. In addition, Umkehr data during high stratospheric aerosol optical depth periods (> 0.025 corresponding to ~ 1 year after El Chichon and ~1 year after Mount Pinatubo) are omitted from the analyses. However, trends calculated with the high-aerosol periods included are not appreciably different from the trends calculated with the high-aerosol periods omitted.

Method 2 is the aerosol-correction method employed by G. Reinsel. This method uses an empirical statistical model approach in which transformed stratospheric optical thickness (transmission) data serve as an exogenous explanatory variable for the Umkehr measurements. The stratospheric aerosol optical thickness data derive from SAGE-II satellite information for the period 1985-1998. For the calculations reported here, these data were appended to the optical thickness data based on composite lidar and SAGE-II measurements through December 1984 used by *Reinsel et al.* [1994]. Thus, in this statistical approach, an additional term, $\gamma_3 Z_{3,t}$, appears in the statistical model described in section 2, where $Z_{3,t} = \exp[-\text{tau}(t)] - 1 \sim -\text{tau}(t)$, where tau($t$) is the optical thickness. We also note that Umkehr data were not used in the estimation for the most extreme aerosol contamination periods (essentially, whenever optical thickness tau(t) > 0.05, i.e., $Z_{3,t} < -0.05$), roughly November 1982 to June 1983 and November 1991 to January 1993 (for 40^0-50^0N).

On the basis of the close correspondence of the results of the three historically used correction methods for the aerosol conditions considered here, we conclude that the corrected Dobson Umkehr ozone data possess less than ~2% residual bias in absolute ozone value due to the aerosol interference in the worst case immediately after the 1-year omitted periods following El Chichon and Mount Pinatubo eruptions. The two independent Umkehr time series analyses both report trends for Umkehr stations Arosa, Boulder, and Haute Provence from 1978 to 1998 (1984-1998 at Haute Provence). These stations were chosen as a result of extensive examination of all Umkehr time series [*WMO*, 1998; *Cunnold et al.*, 2000b]. At each of these stations, both groups computed trends for total-column ozone, for aggregate Umkehr layers 1+2+3+4; individual layers 4, 5, 6, 7, and 8; and aggregate layers 8+9+10. The two independent trend results from the northern midlatitude (40^0-52^0N) stations Arosa, Boulder, and Haute Provence are within 1 standard deviation in all layers. The results reported here are the averages of those two independent analyses.

Extensive comparisons of SAGE I/II and Dobson Umkehr ozone profiles by *Newchurch et al.* [1998] indicate significant temporal correspondence in individual layers 4 through 8. While that study identified a significant bias between SAGE and Dobson Umkehr increasing from 0% in layer 4 to 15% in layer 8 (SAGE higher), the researchers found no evidence of a time dependence in the bias for the stations analyzed in this trend paper.

3.2. Trend Analyses of Dobson Umkehr, SAGE I/II, and SBUV(/2)

We use the Boulder Dobson Umkehr time series from 1979 to 1998 at 40-km in layer 8 (Figure 2a) to illustrate the general analysis process. The Umkehr observations were retrieved with the *Mateer and DeLuisi* [1992] inversion method. These monthly ozone averages, reported in Dobson Units (DU) in the layer, are corrected for aerosol interference throughout the entire time period

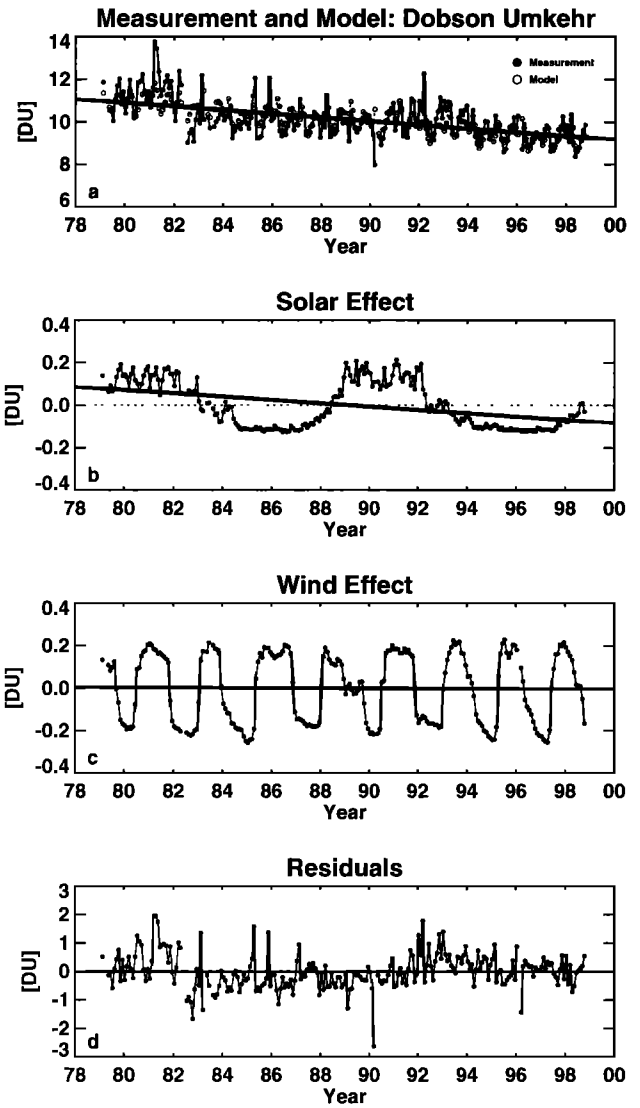

Figure 2. (a) Time series of Dobson Umkehr ozone at Boulder (solid circles) in layer 8 along with the statistical model values (open circles) and the derived trend. (b) Residuals of the statistical model fit to the monthly data. (c) Time series of the solar effect on ozone that the model calculates along with the trend in that solar effect that the model removes from the ozone trend. (d) Time series of the QBO effect on ozone along with the QBO trend.

using the *Mateer and DeLuisi* [1992] factors in the method discussed by *Newchurch and Cunnold* [1994]. Figure 2a displays the measured time series of monthly values as solid circles and the full statistical-model calculations as open circles. Figure 2b displays the solar effect in Dobson Units and the calculated trend in that solar effect that is removed from the final ozone trend. These solar-effect trends are obviously the result of a nonsymmetric solar interval that corresponds to the time interval chosen for evaluation but are entirely accounted for by the statistical model. The QBO effect appears in Figure 2c along with its negligible trend. The most rigorous metric of the statistical model's adequacy is the pattern of the residuals. These residuals appear in Figure 2d. One may see by inspection that neither trend nor temporal pattern related to the exogenous variables remains in the residual series. The magnitude of the random fluctuations about zero is rigorously quantified in the confidence intervals (error bars) reported below on the various trend estimates.

We likewise applied the Newchurch and Yang model to the layer 8, 40^0-50^0N SAGE I/II time series shown in Figure 3 and the layer 8 40^0-50^0N SBUV(/2) time series from 1979 to 1994 in Figure 4. The SAGE I/II observations in Figure 3 are monthly averages of version 5.96 ozone retrievals in a 5-km thick layer between 38-43 km between latitudes 40^0-50^0N. *Cunnold et al.* [2000a] critically address the uncertainties in this data product. This data version is also extensively discussed in the *WMO* [1998] assessment report. The SAGE ozone averages shown here, which include both sunrise and sunset occultation measurements, are reported in the SAGE units of ozone number density versus geometric altitude. In the NIMBUS 7 SBUV version 6 and NOAA 11 (N11) SBUV/2 version 6.1.2 daily average, 50 zonal means are filtered to eliminate data taken at extreme solar-zenith angles as a result of the N11 drifting orbit; then 100 monthly zonal means are created from these data. The monthly mean SBUV(/2) ozone data are reported in Dobson Units within individual Umkehr layers.

Two significant consistencies emerge from the three separate time series viewed together. First the significant ozone decrease between the SAGE I and SAGE II time periods (1982-1984) is supported by decreases of similar magnitude (~10%) in both the Umkehr and SBUV(/2) observations. Second the amplitude of the

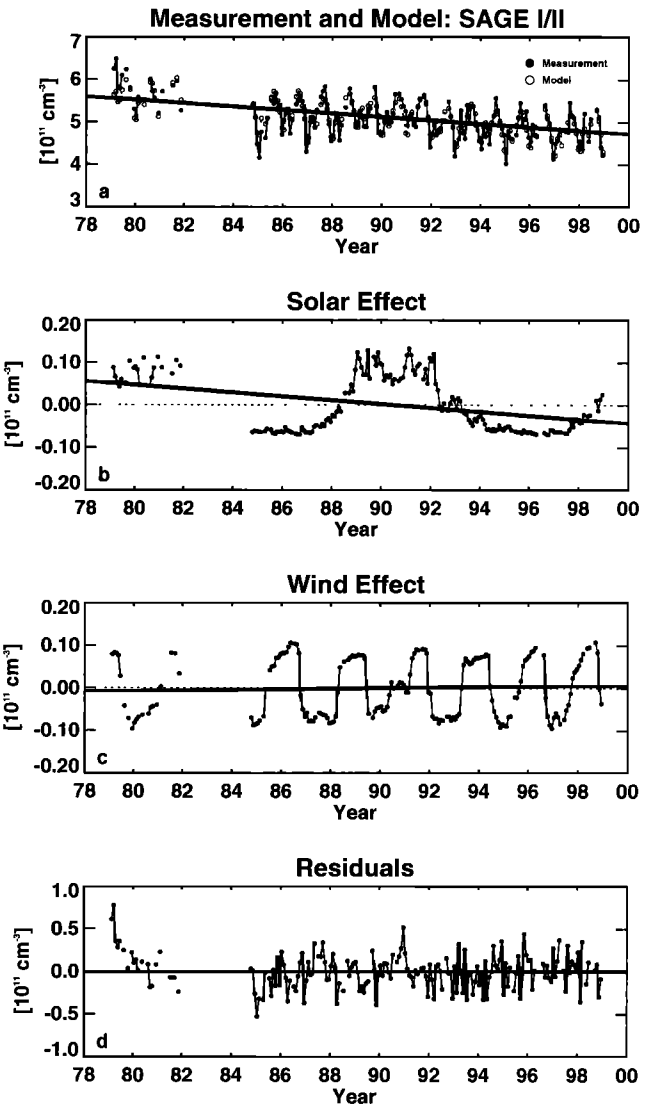

Figure 3. As in Figure 2, except for layer 8, 40^0-50^0N, SAGE I/II ozone.

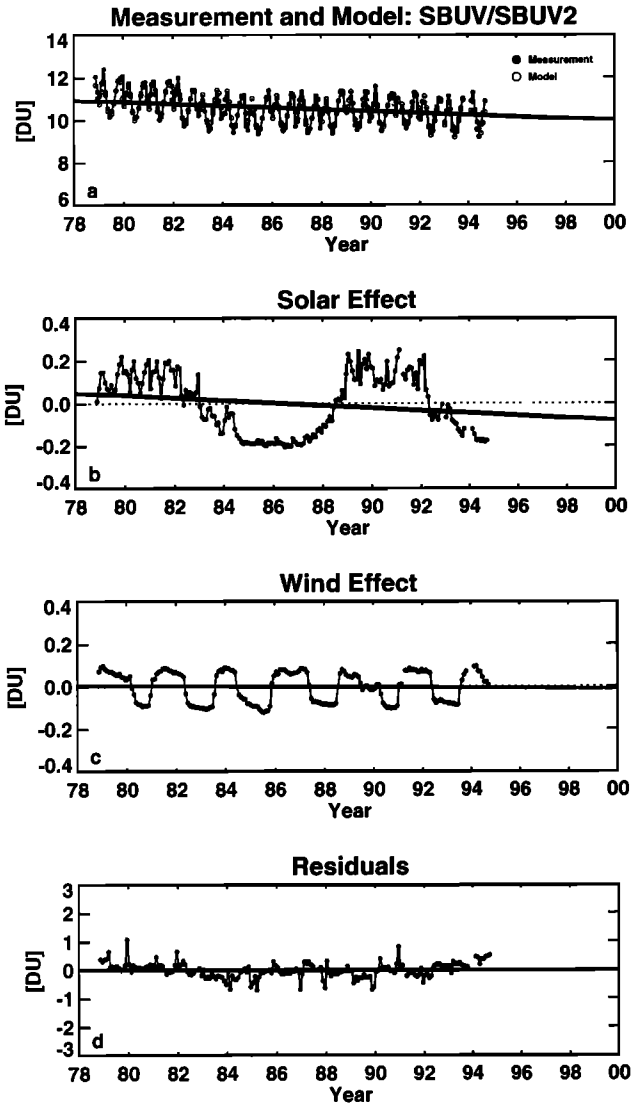

Figure 4. As in Figure 2, except for layer 8, 40^0-50^0N, SBUV(/2) ozone.

annual variation is similar for all three sensors. The correspondence of these three independent ozone time series (with some concern about the SBUV/2 data) suggests that we should have considerable confidence in the trends computed from these data and should expect them to return similar results.

Because of the previous demonstration of the similarity in results of the four statistical models used here, one may conclude that the results of this particular model would have been produced by the other models as well. These measurements are all analyzed and presented in their native units to avoid uncertainties introduced by conversion errors. The magnitude and temporal pattern of the solar effect is essentially the same for all three sensors, as it should be. The temporal evolution of the QBO effect is very similar for all three sensors, although the magnitude of the effect on the SBUV(/2) observations is only half the effect on the Umkehr and SAGE measurements for unknown reasons. In all cases, however, the QBO effect on the resulting ozone trend is essentially zero, as evidenced by the QBO trend lines in Figures 2c, 3c, and 4c that are almost indistinguishable from the zero line. One could argue that the model residuals do not all represent white noise processes (i.e., are not entirely random). For example, the residuals prior to 1981 lie predominantly above zero, although less so for the Umkehr series. The values between 1982 and 1990 in the SBUV(/2) and Umkehr series are predominantly negative, while the 1992-1995 values are mostly positive. The SAGE II 1986-1999 values, however, are randomly distributed about zero. Therefore one could argue that an individual instrument time series suggests a fit of order higher than linear, but if one takes these three series as independent realizations of the true atmosphere (as we have here), then they do not jointly justify a fit of order higher than linear. As a result, the individual linear trends are not perfect, but they are parsimonious.

To show that seasonal variation change has little effect on annual trend estimates in this study, we estimated seasonal amplitudes from TOMS test data, SBUV, and Umkehr measurements at Arosa. We use eight harmonic (12-, 6-, 4-, and 3-month sine and cosines) terms to represent the seasonal variation, instead of using only 12-month sine and cosine harmonics because, at 40 km, 6–, 4–, and/or 3-month harmonic terms are also significant. Analysis of the maximums and minimums of 2-year moving averages indicates small long-term changes in the seasonal amplitude in the TOMS, SBUV, and Dobson Umkehr records. These changes of seasonal amplitude may be real or may be caused by systematic drifts of temperature and ozone measurements, but they do not appear to be statistically significant. However, the topic is beyond the scope of this article. While there is a possibility of the long-term change of seasonal amplitude in ozone measurements, the annual trend estimates in this study are not influenced by the seasonal amplitude change, although those changes may affect seasonal trend estimates. This result is not surprising because the frequency associated with a linear trend is orthogonal to the frequency of the seasonal cycles.

A concern about the SBUV/2 data arises from the large trend differences between SAGE and SBUV/2 ~1% yr^{-1}) reported by *Cunnold et al.* [2000a] that are much bigger than the differences in trends between SAGE and other instruments, and the known potential calibration problems for SBUV/2 arising from its precessing orbit. Recent evaluation of NOAA 11 SBUV/2 ozone profiles using ground-based lidars and microwaves agrees with indications from SAGE II that the NOAA 11 data contain a positive drift (i.e., values increasing relative to the correlative measurements) over the domain 20-45 km. These SBUV/2 uncertainties are reflected in the following discussions, and significantly less weight is given to ozone trend estimates from SBUV/2 in the final combined ozone trend estimates reported in this paper.

3.3. Altitude Profiles of Trends From Umkehr, SAGE I/II, and SBUV(/2)

Applying the statistical models to Dobson Umkehr, SAGE I/II, and SBUV(/2) time series from 1979 (November 1978 for SBUV(/2)) to 1998 (1994 for SBUV(/2)) at 40^0-50^0N in various layers and combinations of layers, while accounting for the potential QBO and solar effects, produces the ozone annual trends in Figure 5, as percent per year (% yr^{-1}) relative to the mean of the period. For Umkehr observations we compute trends for layers 4-8 individually, and for all layers above seven, 8^+, plotted as a vertical bar from ~37 to 54 km. The Umkehr trends in Figure 5 are simple averages of the two group analyses with root-mean-square 2σ error bars. Each individual-group average, however, is a variance-weighted mean. SAGE I/II trends (diamonds) are computed in concentration-versus-altitude coordinates, for individual 1-km layers from 25-50 km but are not all plotted because those 1-km results essentially form a smooth curve through the trends computed for 5-km thick layers corresponding to the Umkehr layers. Trends from SBUV(/2) (circles) are calculated from weekly averages (three daily values required to create a weekly average) and are reported for layers 5-9 individually. All error bars represent

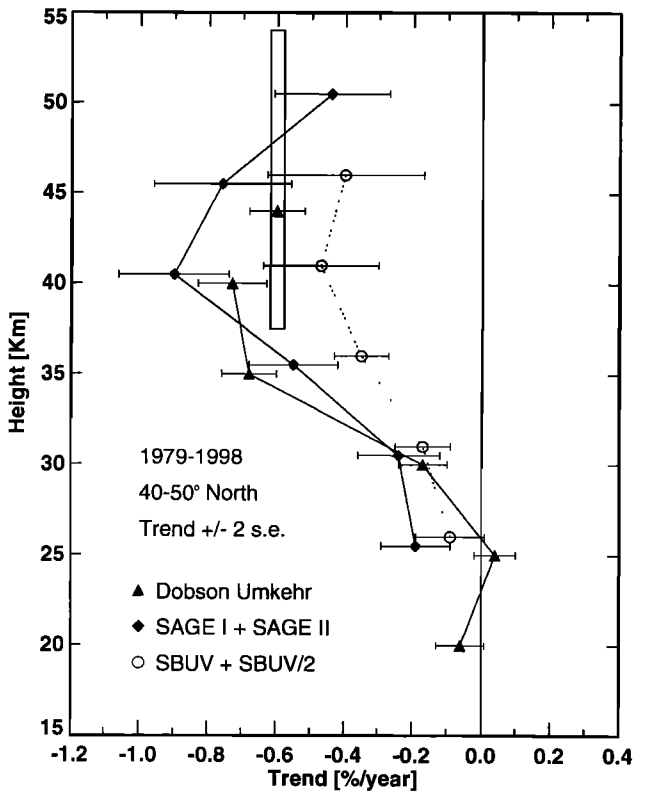

Figure 5. Ozone trends (% yr^{-1} relative to the mean for the period) at 40^0-50^0N over the period 1979-1998 calculated from the following measurement systems: Three Dobson Umkehr stations (Arosa, Boulder, and Haute Provence) reported at individual layers 4 through 8 (triangles) and layers 8+9+10 (plotted as a vertical bar from ~37 to 54 km with triangle); SAGE I/II average sunrise and sunset observations (diamonds) reported at individual layers 4-10; SBUV+SBUV/2 weekly averages (circles) reported at individual layers 5 through 9. All error bars are 95% confidence intervals of the trend and represent statistical uncertainty only. Small vertical offsets are for clarity only (e.g., all values plotted near 30 km represent layer 6 results).

the 2σ statistical-only confidence intervals. Various instrumental uncertainties are estimated in section 3.7, below.

In the upper stratosphere (i.e., layer 8), trend estimates range from -0.5±0.2%yr^{-1} for SBUV(/2) (circles) to –0.9±0.2% yr^{-1} for SAGE I/II (diamonds). The Dobson Umkehr trends for layers 8 and 8^+ are both the intermediate SAGE I/II and SBUV(/2) trends and have somewhat smaller error bars. The 2σ confidence intervals overlap for the SAGE and Dobson sensors and independently for the SBUV(/2) and Dobson sensors, suggesting that the average layer-8 trend of approximately -0.7±0.2% yr^{-1} is a reasonable estimate of the true atmospheric ozone decline at 40 km. A rigorous calculation is presented below.

The similarity between the independent instruments in the trends' vertical structure provides additional confidence that the true trend in atmospheric ozone is being measured. The largest decline occurs near layer 8, and the minimum trend is in layer 5 (~25 km), where the trend estimates range from 0.0±0.1% yr^{-1} by Dobson Umkehr to -0.2±0.1% yr^{-1} by SAGE I/II with the SBUV(/2) results falling between these two values. These results suggest a layer 5 trend of -0.1±0.2% yr^{-1}, which is not significantly different from zero. In layer 9, the SAGE I/II trend is -0.8±0.2% yr^{-1} while the SBUV(/2) estimate (over the shorter period through 1994) is -0.4±0.2 %/yr. The larger SAGE I/II error bars at 45-50 km altitude result primarily from uncertainties due to unresolved trend differences between sunrise and sunset observations.

For trends calculated from all sensors over the SBUV-only time period of 1979-1989, the general altitude structure is much the same as that calculated for the longer time period. The layer 8 average trend is -0.8±0.3% yr^{-1}, resulting from similar estimates from all three sensors. The other layers are not appreciably different from the longer-period trends. The confidence intervals are generally larger because of the shorter time period.

3.4. Latitudinal Trends From SAGE and SBUV(/2)

The latitudinal coverage for the SAGE I/II observations extends from 55^0S to 55^0N. Calculating trends over the period 1979-1998, which comprises the entire SAGE I/II measurement set, results in the altitude-latitude contour plot in Figure 6. These trends are based on concentration changes in 1-km altitude layers (the natural coordinates for SAGE) and are referenced to the concentrations at the midpoint of the time series. Typical uncertainties on the annual trends are 0.2-0.3% yr^{-1} (95% confidence limits). The altitude structure of the trends in layers 4-8 is essentially the same as reported in the WMO report over the shorter time period; however, the area of significant trends is much larger in Figure 6 because of the longer time period and because of a correction for an inadvertent error in accounting of the uncertainty resulting from the SAGE sunrise/sunset trend differences.

In this global view the maximum ozone trends remain at 40 km (layer 8) but are larger in the extra tropics (-1.0% yr^{-1}) than in the tropics (-0.6% yr^{-1}). The minimum trend in layer 5 occurs at all latitudes with no positive trends in the tropics as were reported by *WMO* [1998]. In general, the SAGE I/II trends are significantly different from zero, at the 95% confidence level (approximately ±0.2% yr^{-1}), and at all latitudes outside of the tropics for altitudes above layer 6 (30 km). The trends exhibit remarkable hemispheric symmetry except in layers 4 and 5 for latitudes poleward of 40^0.

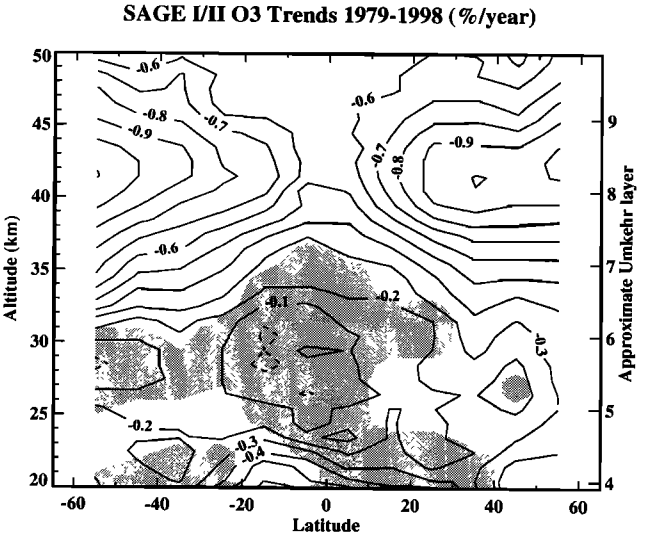

Figure 6. Annual ozone trends calculated from SAGE I/II observations from 1979 to 1998 expressed in % yr^{-1} of the midpoint of the time series (1989). Results are contoured from calculations done in 50 latitude bands and 1-km altitude intervals. Contours differ by 0.1% yr^{-1} with the solid contours indicating zero or negative trend. The shaded areas indicate where the trends do not differ from zero within 95% confidence limits. The estimate of uncertainty contains terms due to statistical uncertainty, the SAGE-I reference height correction, and the SAGE II sunrise/sunset trend differences.

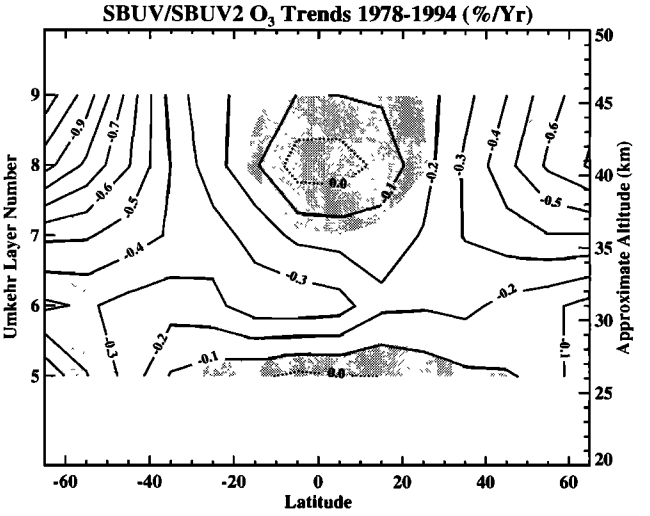

Figure 7. Annual SBUV+SBUV/2 trend calculated from November 1978 through October 1994 as a function of latitude and Umkehr layer. The trend is in % yr^{-1} relative to the mean ozone amount from the combined time series at each latitude and layer. The dark shading indicates the regions in which the derived trend is not significantly different from zero at the 95% confidence level calculated from statistical uncertainty only; inclusion of the instrument error renders no statistically significant trends between 35°S and 45°N. The lighter shading at high northern and southern latitudes indicates regions in which the length of the time series during the winter season is compromised as a result of the NOAA 11 orbit drift (taken from *WMO* [1998, Figure 3.18].

Figure 7 shows the SBUV(/2) trends from November 1978 to October 1994 in % yr^{-1} relative to the mean ozone amount from the combined time series at each latitude and layer. The dark shading indicates the regions in which the derived trend is not significantly different from zero at the 2σ level calculated from statistical-only error bars; inclusion of the instrument error gives no statistically significant trends between 35°S and 45°N at the 2σ level. The lighter shading indicates regions in which the length of the time series during the winter season is compromised as a result of the NOAA 11 orbit drift. Therefore, at these latitudes, the true annual average trend for 1978-1994 cannot be calculated. In the Northern Hemisphere the data loss is not as extensive as in the Southern Hemisphere; therefore the northern high-latitude trends are more representative of the true annual average trends over this time period. In contrast, data loss in the Southern Hemisphere high latitudes begins as early as 1990, such that the trends plotted here are actually an average of the spring, summer, and autumn trends through 1994 and the winter trend through 1990. The largest ozone losses occur during winter in the profile data through 1990. Thus we expect an increased uncertainty in the middle- to high-latitude annual average trends in the Southern Hemisphere over this time period. Comparing the SAGE I/II trends in Figure 6 to the SBUV(/2) trends in Figure 7 indicates similarly small trends of 0.0 to -0.3% yr^{-1} in layers 5 and 6. In the upper stratosphere, the altitudinal and latitudinal structures of the SAGE I/II and SBUV(/2) trends are similar; however, the SAGE I/II trends are substantially more negative at nearly all latitudes.

The principal difference between the SAGE I/II trends from 1979 to 1998 and the SBUV(/2) trends from 1979 to 1994 should be ascribed to the SBUV/2 problems (as indicated by *Cunnold et al.* [2000a]). SAGE I altitudes have been adjusted as per *Wang et al.* [1996], and the uncertainties in those adjustments have been included in the SAGE trend error bars. Altitude registration uncertainties between SAGE I and SAGE II in the upper stratosphere are not large enough to contribute substantially to these differences. SAGE trends are presented on altitude surfaces whereas SBUV trends are on pressure levels. Neither of these trend results is affected by temperature uncertainties. However differences between the two sets of trends might be interpreted as resulting from long-term temperature/geopotential height trends. The largest reported trends in the National Centers for Environmental Prediction (NCEP) data are in the tropics in the upper stratosphere. These amount to ~300m over the 15-year period or equivalently to a trend in ozone of ~0.4% yr^{-1} (based on an ozone scale height of 5 km). However, a recent reanalysis of the NCEP data as well as an analysis of SAGE Rayleigh scattering data suggests that the geopotential height change is significantly smaller than this.

3.5. Seasonal Trends

Investigating the layer 8 trends as a function of latitude and month, we find that the SAGE I/II (Figure 8) results show a minimum trend of –0.7% yr^{-1} in the Northern Hemisphere summer and a maximum of –1.2% yr^{-1} in the winter (i.e., ±30%). The Southern Hemisphere midlatitude results are –0.5 to –1.2% yr^{-1} (±40%). SBUV(/2) (Figure 9) indicates seasonal variation from -0.2% yr^{-1} in Northern Hemisphere summer to –0.6% yr^{-1} in winter. The Southern Hemisphere variation is somewhat larger. The magnitude and structure of the ozone trends' seasonal variation are similar to the results given by *WMO* [1998]; however, the area of insignificance in Figure 8 is approximately half the area of the corresponding results in the WMO report. That report inadvertently considered 1/2 the sunset/sunrise trend differences to be the 95% confidence interval limit. In this paper, as was intended in the WMO report, we consider 1/4 of the sunset/sunrise trend difference to be the 95% limit [see, also, *Cunnold et al.*, 2000a]. The zonal seasonal variations average over the longitudinal differences in seasonal variation. The winter-hemisphere trend maximum in the upper stratosphere is clearly evident in the SAGE I/II seasonal-trend cross sections; the equinox patterns show more symmetry between hemispheres. This seasonal pattern seen in the satellite data is consistent with results from the Dobson Umkehr analyses at the Arosa, Boulder, and Haute Provence northern midlatitude stations and the Perth and Lauder southern midlatitude stations.

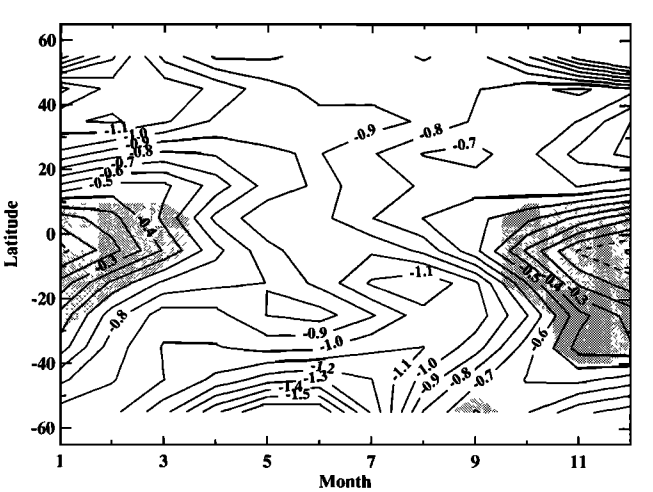

Figure 8. Seasonal variation of ozone trends in layer 8 (% yr^{-1}) calculated from SAGE I/II (version 5.96, 1979-1998) for latitudes 55°S to 55°N. Shading indicates 95% confidence intervals that include statistical uncertainties, uncertainties due to SAGE-I altitude correction, and SAGE II sunrise/sunset differences.

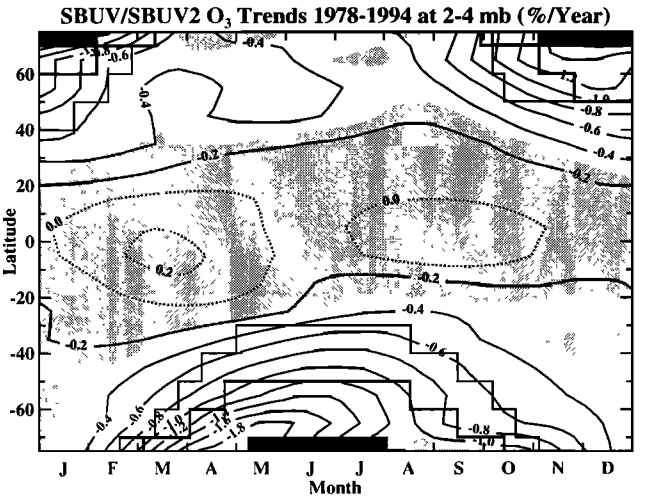

Figure 9. Seasonal variation of ozone trends in layer 8 (% yr^{-1}) calculated from SBUV (version 6) and SBUV/2 (version 6.1.2) (1978-1994). The shading indicates 95% confidence intervals from statistical errors only. The solid black shading indicates regions of no data due to polar night. The thick black line surrounding polar night designates the regions with no SBUV/2 data because of the drifting NOAA 11 orbit; the thin black line designates the regions with no SBUV/2 data after 1992 due to continuing drift of the orbit. In 1994, there are no data in the Southern Hemisphere outside of the tropics after about April (taken from *WMO* [1998, Figure 3.22].

The seasonal variation of the Umkehr trends is somewhat smaller than seen in SAGE and the limited number of Umkehr stations in the Southern Hemisphere provide limited constraint on these seasonal trends. Near 40° in the Northern Hemisphere, the SAGE I/II negative-trend minimum occurs in the late winter while the SBUV(/2) (Figure 9) negative-trend minimum occurs two months earlier, in the early winter, and does not show the significant tropical trends between April and September.

Seasonal variations calculated by the Goddard Space Flight Center (GSFC) two-dimensional model [*Considine et al.*, 1998] are much smaller than all of the results reported here, especially in the tropics and Southern Hemisphere. One could argue that the 2σ uncertainty in the SAGE and SBUV trends is of the order of -0.4% yr^{-1} and therefore variations of ±0.4% yr^{-1} seen, for example, in the SAGE northern midlatitude results are at best marginally significant. Further study will be needed to resolve this issue.

3.6. Hemispheric Symmetries in 40-km Trends From SAGE and SBUV(/2)

In order to test for the presence of an interhemispheric asymmetry in the ozone trend, we focus on layer 8 and inspect the ozone trends as a function of latitude. In none of the three periods, the layer 8 SAGE I/II trends as a function of latitude for the first 11 years (1979-1990), the last 14 years (1984-1998), and all 19 years (1979-1998), is an interhemispheric difference in the trends statistically significant. Although interhemispheric differences exist in the mean results for both SBUV and SAGE I/II in the first 11-year period, these differences are not statistically significant. In layer 9, the N7 SBUV trend asymmetry is ~0.5% yr^{-1}, but it is still not statistically significant due to large interannual variability at high latitudes. The interhemispheric symmetry found here with updated time series and analysis does not change the conclusion of *WMO* [1998].

3.7. Combined Instrument Drift and Statistical Uncertainty Estimates

Each individual instrument-trend calculation presented above possesses an associated estimate of the statistical uncertainty. However, an additional uncertainty, owing to the potential drift of the instrument system over time, was not reflected in those confidence intervals in part because it is difficult to quantify such errors uniformly over the various experiments. An attempt at quantifying these instrument-drift uncertainties is reported by *WMO* [1998] and *Cunnold et al.* [2000a] (reported here in Table 1, column "Inst, % yr^{-1}"). This section combines those potential instrument-drift uncertainties with the estimates for the statistical sampling uncertainty (Table 1, column "Stat, % yr^{-1}") from the time series models. This combination results in an estimate of the overall uncertainty for each of the instrument systems.

The SAGE I/II results include instrumental error estimates attributable to the SAGE-I altitude correction, sunrise/sunset trend differences (important above layer 7), and other errors specified in Table 1.1 of *WMO* [1998]. The SAGE error bars in the upper stratosphere reflect a different accounting of the disparity between SAGE sunrise observation trends and sunset trends compared to the accounting by *WMO* [1998], as described in this section. Those smaller confidence limits are reflected in smaller error bars on the SAGE trends reported here compared to the *WMO* values. The SBUV(/2) trend error bars derive from both calibration and algorithm errors summarized in Table 1.8 and Umkehr error sources follow Table 1.12 of *WMO* [1998].

The *WMO* [1998] Ozone Trends Assessment Report combined the individual instrument and statistical uncertainties in a root-sum-square (RSS) approach. In Table 1, column "RSS(Stat, Inst), % yr^{-1}," we report an analogous quantity; however, the Table 1 SAGE values are smaller than those in the WMO [1998] report. The Table 1 estimates reflect the SAGE sunrise/sunset trend differences as contributing only half of the magnitude erroneously reported before. The time series is also 2 years longer for SAGE and Umkehr, reducing the statistical uncertainty. In this paper we also present an upper bound to combining instrument and statistical uncertainties by considering the individual instrument and sta-

Table 1. Trends and Uncertainties for Each Independent Measurement System for Northern Midlatitudes

Alt, km	Trend % yr^{-1}	Stat, % yr^{-1}	Inst, % yr^{-1}	RSS (Stat, Inst) % yr^{-1}	Stat+Inst, % yr^{-1}
			SAGE I/II		
50	-0.44	.17	.32	0.36	0.49
45	-0.76	.20	.20	0.28	0.40
40	-0.90	.16	.14	0.22	0.30
35	-0.55	.13	.10	0.17	0.23
30	-0.24	.12	.22	0.25	0.34
25	-0.19	.10	.28	0.30	0.38
			SBUV(/2)		
45	-0.40	.23	.50	0.55	0.73
40	-0.47	.17	.50	0.53	0.67
35	-0.35	.08	.48	0.49	0.56
30	-0.17	.08	.40	0.41	0.48
25	-0.09	.10	.30	0.32	0.40
			Dobson Umkehr		
40	-0.73	.10	0.46	0.47	0.56
35	-0.68	.08	0.42	0.43	0.50
30	-0.17	.07	0.40	0.41	0.47
25	0.04	.06	0.40	0.40	0.46

All uncertainties are given as 2σ.

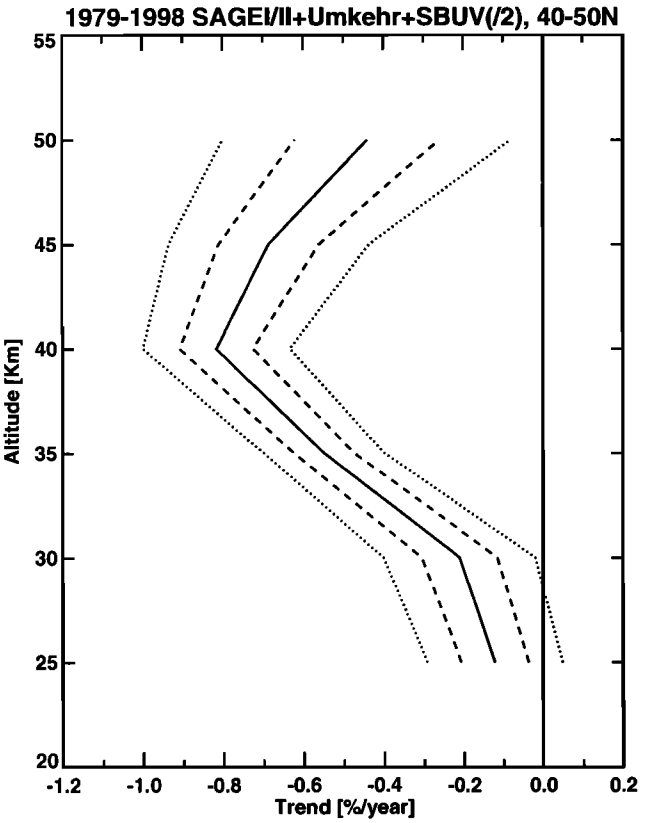

Figure 10. Estimate of mean ozone trend (% yr^{-1}) using variance-weighted estimates from Dobson Umkehr, SAGE I/II, and SBUV(/2) at 40^0-50^0 north (thick solid line). Combined uncertainties are also shown as 1σ (dashed line) and 2σ (dotted line).

tistical uncertainty terms as additive. Because of the significantly smaller SAGE error reported here at 50 km due to the discounting of the sunrise/sunset trend discrepancy, that sum (Table 1, column "Stat+Inst, % yr^{-1}") results in a smaller uncertainty compared to the error estimate resulting from the RSS approach reported by *WMO* [1998]; the individual-sensor mean-trend estimates, of course, remain the same regardless of the method employed for error calculation. We also combine the SAGE I/II, SBUV(/2), and Dobson Umkehr trends and uncertainties, assuming they are three independent estimates of the same trend by computing a weighted mean and an RSS error estimate from those three sensors. The weights are the inverse square of the instrument and statistical errors for each sensor, respectively. Table 2 gives the result for each of the systems for northern mid latitudes (40^0-50^0N). The trends and error estimates reported by *WMO* [1998] appear in the second and third columns, respectively, of Table 2, while the trend results of this study, the analogous RSS error estimate, and also the upper-bound sum of the statistical and instrument errors appear in the last three columns, respectively. The weighted mean trends do not differ appreciably between the two methods; however, the RSS error estimates calculated here are significantly smaller at 50 km compared to the *WMO* [1998] error estimates because of the smaller estimated contribution from the sunrise/sunset trend differences. The upper-bound estimates are marginally larger at all altitudes except at 50 km due to smaller statistical uncertainties associated with these longer time series and the sunrise/sunset error difference at 50 km. The true uncertainty probably lies between the two values reported here.

Figure 10 shows the three-sensor-combined mean trend enveloped by both one and two standard errors calculated as RSS of statistical and instrument errors (Table 2, column 5). The trends for the upper stratosphere are dominated by those determined from the SAGE instruments because these instruments have the smallest estimated uncertainty. The result of this trend estimation at 40 km is -0.82% yr^{-1} ±0.18 % yr^{-1} (2σ), a highly significant trend. The trend at 50 km is estimated from the SAGE instruments only and is also significant at the 95% confidence level. Because the -0.12% yr^{-1} trend at 25 km reported here does not include the trend estimate from the ozonesonde network analysis, it is not as negative as the *WMO* [1998] or *Randel et al.* [1999] estimate of –0.3% yr^{-1}, which includes the more negative estimate from the sonde network.

4. Conclusions

Comparison of 10 different statistical modeling efforts applied to identical ozone time series indicates that trends calculated for continuous series with no missing values are essentially identical across all models (i.e., ±0.015% yr^{-1} (1σ)). These results are reported in detail by *WMO* [1998, 1999]. Worst-case comparisons from a time series with significant missing data and poorly sampled seasons results in agreement of 0.2% yr^{-1} at the 1σ level. This level of agreement is comparable to the confidence interval associated with an individual model's trend estimate of the same time series. Details of the terms and construction of an individual model (e.g., the assumptions associated with the autoregressive coefficient calculation or with the formulation of the exogenous explanatory series) affect the resulting confidence interval more than those assumptions affect the computed trend value.

Similarities between measurements of northern midlatitude ozone trends at 40-km altitude from 1979 to 1998 by three independent sensor systems (Dobson Umkehr, SAGE I/II, and SBUV plus SBUV/2 (SBUV/2 until 1994)) provide high confidence in the accuracy of these ozone time series. All three sensor systems record similar annual variation amplitudes. As demonstrated by the residuals of the statistical model, this temporal behavior is reasonably well described by the simultaneous effects of solar varia-

Table 2. Weighted Mean Trends and 2σ Uncertainties From the SAGE I/II, SBUV(/2), and Dobson Umkehr Observations Combined

Alt	IOC/SPARC Three-system Weighted Mean Trend % yr^{-1}	IOC/SPARC 2σ RSS [RSS(Stat,Inst)] % yr^{-1}	Three-system, Weighted Mean Trend % yr^{-1}	2σ RSS [Σ(Stat, Inst)] % yr^{-1}	2σ RSS [Σ(Stat+Inst)] % yr^{-1}
50	-0.45	0.82	-0.44	0.36	0.49
45	-0.60	0.33	-0.69	0.25	0.35
40	-0.74	0.20	-0.83	0.18	0.25
35	-0.50	0.18	-0.54	0.15	0.20
30	-0.20	0.23	-0.21	0.19	0.24
25	-0.10	0.20	-0.11	0.19	0.24

tion and a linear trend consistent with the monotonic increase of stratospheric chlorine.

Two independent analyses of the Dobson Umkehr observations report very similar ozone trends and indicate less than 2% residual error due to aerosol optical interference when the years following the El Chichon and Mount Pinatubo eruptions are omitted. Problems resulting from the drifting orbit of the SBUV/2 satellite and from instrument calibration reduce our confidence in the magnitude of the trends derived from SBUV/2 observations [see *Cunnold et al.*, 2000a].

Taken together, the Dobson Umkehr, SAGE I/II, and SBUV(/2) zonal mean profiles of trends at 40^0-50^0N indicate maximum negative trends of -0.8±0.2% yr^{-1} (2σ statistical uncertainty) at 40 km and minimum negative trends of -0.1±0.2% yr^{-1} (2σ statistical uncertainty) at 25 km with substantial agreement between the three sensors. Meridional cross sections of SAGE I/II and SBUV(/2) exhibit north-south symmetry in upper stratospheric trends with minimum values in the tropics and maximum values at midlatitudes. All three sensors also show good agreement in the vertical structure of the ozone trends. The satellite data indicate a 30-40% seasonal variation in the zonal midlatitude trends (most negative in the winter), while the Dobson Umkehr results indicate somewhat less seasonal variation. Some of this difference may be attributable to the zonal averaging of the satellite data versus the longitude-specific location of the ground-based observations. Both SAGE I/II and SBUV(/2) show no statistically significant north-south hemispheric asymmetry in the upper stratosphere ozone trends over this period.

Combining the trends from all three sensor systems as a weighted mean that accounts for an estimate of the instrument-drift uncertainty in addition to the statistical-trend uncertainty indicates significant ozone decline from 1979-1998 throughout the upper stratosphere.

Acknowledgments. We wish to thank Lucien Froidevaux, Johannes Staehelin, Pierre Viatte and two anonymous reviewers for constructive suggestions. Portions of this work, including work at the University of Alabama in Huntsville and the University of Arizona, were supported by the NASA Atmospheric Chemistry Modeling and Analysis Program. We wish to acknowledge Jack Kaye/NASA/HQ for the initiation and support of the WMO Ozone Trends Assessment effort. Dobson Umkehr data were provided by Ed Hare at the World Ozone Data Centre and by Gloria Koenig at NOAA/CMDL. SAGE data were provided by Joe Zawodny at NASA/LaRC and the SAGE Science Team. Additional aerosol data for the Umkehr correction were provided by Horst Jäger at the Fraunhofer Institute for Atmospheric Environmental Research, Garmisch-Partenkirchen. Reprocessed SBUV/2 data were obtained from NOAA/NESDIS with support from the NOAA Climate and Global Change Program Atmospheric Chemistry Element.

References

Aellig, C.P., et al., Latitudinal distribution of upper stratospheric ClO as derived from space borne microwave spectroscopy, *Geophys. Res. Lett., 23*, 2321-2324, 1996.

Bojkov, R., L. Bishop, W.J. Hill, G.C. Reinsel, and G.C. Tiao, A statistical trend analysis of revised Dobson total ozone data over the northern hemisphere, *J. Geophys. Res., 95*, 9785-9807, 1990.

Chandra, S., C.H. Jackman, and E.L. Fleming, Recent trends in ozone in the upper stratosphere: Implications for chlorine chemistry, *Geophys. Res. Lett., 22*, 843-846, 1995.

Considine, D.B., A.E. Dessler, C.H. Jackman, J.E. Rosenfield, P.E. Meade, M.R. Schoeberl, A.E. Roche, and J.W. Waters, Interhemispheric asymmetry in the 1 mbar O_3 trend: An analysis using an interactive zonal mean model and UARS data, *J. Geophys. Res., 103*, 1607-1618, 1998.

Cunnold, D.M., M.J. Newchurch, L.E. Flynn, H.J.Wang, J.M. Russell, R. McPeters, J.M. Zawodny, and L. Froidevaux, Uncertainties in upper stratospheric ozone trends from 1979 to 1996, *J. Geophys. Res., 105*, 4427-4444, 2000a.

Cunnold, D.M., H.J. Wang, L. Thomason, J. Zawodny, J.A. Logan, and I.A. Megretskaia, SAGE (v5.96) ozone trends in the lower stratosphere, *J. Geophys. Res., 105*, 4445-4457, 2000b.

DeLuisi, J.J., C.L. Mateer, D. Theisen, P.K. Bhartia, D. Longenecker, and B. Chu, Northern middle-latitude ozone profile features and trends observed by SBUV and Umkehr, 1979-1990, *J. Geophys. Res., 99*, 18,901-18,908, 1994.

Fraser, P.J., D.E. Oram, C.E. Reeves, S.A. Penkett, and A. McCulloch, Southern hemispheric halon trends (1978-1998) and global halon emissions, *J. Geophys. Res., 104*, 15,985-15,999, 1999.

Harris, N.R.P., et al., Trends in stratospheric and free tropospheric ozone, *J. Geophys. Res., 102*, 1571-1590, 1997.

Hollandsworth, S.M., R.D. McPeters, L.E. Flynn, W. Planet, A.J. Miller, and C. Chandra, Ozone trends deduced from combined Nimbus 7 SBUV and NOAA 11 SBUV/2 data, *Geophys. Res. Lett., 22*, 905-908, 1995.

Hood, L.L., R.D. McPeters, J. McCormick, L.E. Flynn, S.F. Hollandsworth, and J.F. Gleason, Altitude dependence of stratospheric ozone trends based on Nimbus 7 SBUV data, *Geophys. Res. Lett., 20*, 2667-2670, 1993.

Jackman, C.H., E.L. Fleming, S. Chandra, D.B. Considine, and J.E. Rosenfield, Past, present, and future modeled ozone trends with comparisons to observed trends, *J. Geophys. Res., 101*, 28,753-28,767, 1996.

Kaye, J. A., and R. B. Rood, Chemistry and transport in a three-dimensional stratospheric model: Chlorine species during a simulated stratospheric warming, *J. Geophys. Res., 94*, 1057-1083, 1989.

Lipson, J. B., M. J. Elrod, T. W. Beiderhase, L. T. Molina, and J. J. Molina, Temperature dependence of the rate constant and branching ratio of the OH + ClO reaction, *J. Chem. Soc. Faraday Trans., 93*, 2665-2673, 1997.

Logan, J.A., et al., Trends in the vertical distribution of ozone: A comparison of two analyses of ozonesonde data, *J. Geophys. Res., 104*, 26,373-26,399, 1999.

Madronich, S., R.L. McKenzie, L.O. Björn, and M.M. Caldwell, Changes in biologically active ultraviolet radiation reaching the Earth's surface, *J. Photochem. Photobiol. B, 46*, 5-19, 1998.

Mateer, C.L., and J.J. DeLuisi, A new Umkehr inversion algorithm, *J. Atmos. Terr. Phys., 54*, 537-556, 1992.

McPeters, R.D., T. Miles, L.E. Flynn, C.G. Wellemeyer, and J.M. Zawodny, Comparison of SBUV and SAGE II ozone profiles: Implications for ozone trends, *J. Geophys. Res., 99*, 20,513-20,524, 1994.

Miller, A.J., G.C. Tiao, G.C. Reinsel, D. Wuebbles, L. Bishop, J. Kerr, R. M. Nagatani, J.J. DeLuisi, and C.L. Mateer, Comparisons of observed ozone trends in the stratosphere through examination of Umkehr and balloon ozonesonde data, *J. Geophys. Res., 100*, 11,209-11,217, 1995.

Miller, A.J., et al., Comparisons of observed ozone trends and solar effects in the stratosphere through examination of ground-based Umkehr and combined solar backscattered ultraviolet (SBUV) and SBUV 2 satellite data, *J. Geophys. Res., 101*, 9017-9021, 1996.

Newchurch, M.J., and D.M. Cunnold, Aerosol effects on Umkehr ozone profiles using SAGE II measurements, *J. Geophys. Res., 99*, 1383-1388, 1994.

Newchurch, M.J., D.M. Cunnold, and H.J. Wang, Stratospheric Aerosol and Gas Experiment II - Umkehr ozone profile comparisons, *J. Geophys. Res., 100*, 14029-14042, 1995.

Newchurch, M.J., D.M. Cunnold, and J. Cao, Intercomparison of SAGE with Umkehr[64] and Umkehr[92] ozone profiles and time series: 1979-1991, *J. Geophys. Res., 103*, 31,277-31,292, 1998.

Randel, W.J., F. Wu, J.M. Russell III, A. Roche, and J.W. Waters, Seasonal cycles and QBO variations in stratospheric CH4 and H2O observed in UARS HALOE data, *J. Atmos. Sci., 55*, 163-185, 1998.

Randel, W.J., R.S. Stolarski, D.M. Cunnold, J.A. Logan, M.J. Newchurch, and J.M. Zawodny, Trends in the vertical distribution of ozone. *Science, 285*, 1689-1692, 1999.

Reinsel, G.C., W.-K. Tam, and L.H. Ying, Comparison of trend analyses for Umkehr data using new and previous inversion algorithms, *Geophys. Res. Lett., 21*, 1007-1010, 1994.

Reinsel, G.C., G.C. Taio, A.J. Miller, R.M.Nagatani, D.J. Wuebbles, E.C. Weatherhead, W.-K. Cheang, L. Zhang, L.E. Flynn, and J. B. Kerr, Update of Umkehr ozone profile data trend analysis through 1997, *J. Geophys. Res., 104*, 23,881-23,898, 1999.

Rusch, D.W., R.T. Clancy, and P.K. Bhartia, Comparison of satellite measurements of ozone and ozone trends, *J. Geophys. Res., 99*, 20,501-20,511, 1994.

Shindell, D.T., D. Rind, and P. Lonergan, Increased polar stratospheric

ozone losses and delayed eventual recovery owing to increasing greenhouse-gas concentrations, *Nature, 392*, 589-592, 1998.

Solomon, S., and R.R. Garcia, On the distribution of long-lived tracers and chlorine species in the middle atmosphere, *J. Geophys. Res., 89*, 11,633-11,644, 1984.

Wang, H.J., D.M. Cunnold, and X. Bao, A critical analysis of SAGE ozone trends, *J. Geophys. Res., 101*, 12,495-12,514, 1996.

Waters, J.W., et al., Validation of UARS Microwave Limb Sounder ClO Measurements, *J. Geophys. Res., 101*, 10,091-10,127, 1996.

World Meteorological Organization, (WMO), *Report of the International Ozone Trends Panel: 1988, rep. 18*, World Meteorol. Org. Global Ozone Res. and Monit. Proj., Geneva, 1989.

World Meteorological Organization, (WMO), *Scientific Assessment of Stratospheric Ozone: 1994, rep. 37*, World Meteorol. Org. Global Ozone Res. and Monit. Proj., Geneva, 1995.

World Meteorological Organization, (WMO), *Assessment of Trends in the Vertical Distribution of Ozone, rep. 43*, Global Ozone Res. and Monit. Proj., Geneva, 1998.

World Meteorological Organization, (WMO), *Scientific Assessment of Ozone Depletion: 1998, rep. 44*, World Meteorol. Org. Global Ozone Res. and Monit. Proj., Geneva, 1999.

L. Bishop, Allied Signal Corporation, 20 Peabody Street, Buffalo NY 14210. (lane.bishop@alliedsignal.com)

D. Cunnold and R. Wang, School of Earth and Atmospheric Sciences Georgia Institute of Technology, Atlanta, GA 30332. (cunnold@eas.gatech.edu)

L. E. Flynn, NOAA/NESDIS, 5200 Auth Road, Silver Spring, MD 20233. (lflynn@orbit.nesdis.noaa.gov)

S. Godin, Service d'Aeronomie, Universite Pierre et Marie Curie, 4 Place Jussieu - boite 102, Tour 15 Couloir 15-14 Paris, France 75252. (sophie.godin@aero.jussieu.fr)

S. Hollandsworth and R. Stolarski, NASA/Goddard Space Flight Center, Code 916, Laboratory for Atmospheres, Greenbelt, MD 20771. (smh@qhearts.gsfc.nasa.gov; stolarski@polska.gsfc.nasa.gov)

L. Hood, Lunar and Planetary Laboratory, University of Arizona, Tucson, AZ 85721. (lon@lpl.arizona.edu)

A. J. Miller, NOAA/National Weather Service, Climate Prediction Center, 5200 Auth Road, Camp Springs, MD 20233. (miller@upair.wwb.noaa.gov)

M. J. Newchurch and E.-S. Yang, Department of Atmospheric Science, University of Alabama in Huntsville, Huntsville, AL 35899. (mike@atmos.uah.edu; yes@atmos.uah.edu)

S. Oltmans, NOAA, Climate Monitoring & Diagnostics Laboratory, 325 Broadway R/CMDL, Boulder, CO 80303. (soltmans@cmdl.noaa.gov)

W. Randel, National Center for Atmospheric Research, Boulder, CO 80307-3000. (randel@ncar.ucar.edu)

G. Reinsel, Statistics Department, University of Wisconsin, Madison, WI 53706. (reinsel@stat.wisc.edu)

(Received September 13, 1999; revised January 13, 2000; accepted January 17, 2000)